Identification of aberrantly methylated-differentially expressed genes and potential agents for Ewing's sarcoma

Shijie Gao
Tianjin Medical University General Hospital
Guowang Li
Tianjin Medical University General Hospital
Hao Yu
Tianjin Medical University General Hospital
Shiyang Yuan
Tianjin Medical University General Hospital
Wenxiang Li
Tianjin Medical University General Hospital
Ziqian Xiang
Tianjin Medical University General Hospital
Wendong Ruan
Tianjin Medical University General Hospital
Guangzhi Ning (ningguangzhi9@163.com)
Tianjin Medical University General Hospital https://orcid.org/0000-0002-9018-1866

Research article

Keywords: methylation, Ewing's sarcoma, bioinformatics, expression

Posted Date: August 28th, 2020

DOI: https://doi.org/10.21203/rs.3.rs-62293/v1

Abstract

Background

DNA methylation is a common epigenetic regulatory way, and it plays a critical role in various human diseases. However, the potential role of how DNA methylation impacts Ewing's sarcoma (ES) is not clear. This study aimed to explore the regulatory role of DNA methylation in ES.

Methods

The microarray data of gene expression and methylation were downloaded from Gene Expression Omnibus (GEO) database, and analyzed via GEO2R. Venn analysis was then applied to identify aberrantly methylated differentially expressed genes (DEGs). Subsequently, Function and pathway enrichment analysis was conducted. Protein-protein interaction (PPI) network was constructed. Hub genes were determined. Besides, a connectivity map (CMap) analysis was performed to screen bioactive compounds for ES treatment.

Results

A total of 135 hypomethylated high expression genes and 523 hypermethylated low expression genes were identified. The hypomethylated high expression genes were enriched in signal transduction and the apoptosis process. Meanwhile, hypermethylated low expression genes were related to DNA replication and transcription regulation. We next determined 10 hub genes through PPI analysis, among them, C3, TF, and TCEB1 might serve as diagnostic and therapeutic targets. Furthermore, CMap analysis revealed 6 chemicals as potential options for ES treatment.

Conclusions

For the first time, we jointly analyzed gene profiling and methylation data about ES. The introduction of DNA methylation characteristics over DEGs is helpful to understand the pathogenesis of ES. The identified hub aberrantly methylated DEGs and chemicals might provide some novel insights on ES treatment.

Background

ES is a malignant tumor that occurs in bone or soft tissue and has a high incidence rate in children and adolescents[1]. ES is highly aggressive and easy to relapse after resection[2]. Despite advanced multidisciplinary therapies, the prognosis of ES patients remains poor[3]. A chromosomal translocation between the *ESR1* gene on chromosome 22 and the *FLI1* gene on chromosome 11 is present in

approximately 85% of ES cases[4]. Besides, epigenetic alterations of tumor suppressor genes and protein-coding proto-oncogenes have greatly influenced the development of ES[5]. For all these reasons, research on the epigenetics of ES is highly demanded for improving clinical outcomes.

Epigenetics is related to changes in gene function but does not involve changes in gene sequences[6]. Several molecular factors, including DNA methylation, non-coding RNA, and histones modification, are important in cancer epigenetics, and aberrant DNA methylation has been the subject of intensive research[7]. Aberrant DNA methylation is common in most tumors and greatly influence the process of tumor evolution by influencing the expression of key genes[8]. Although multiple studies have been performed on aberrant DNA methylation in ES[9], the comprehensive profile of the aberrantly methylated-differentially expressed genes and their roles in the development of ES remain unclear.

Until now, no research has simultaneously analyzed gene expression and gene methylation data and their link to ES development. In the present study, the gene expression profile (GSE45544) and gene methylation profile (GSE118872) were downloaded from the GEO database, and subsequently, a series of bioinformatics analyses were performed. We identified abnormally methylated-differentially expressed genes and their correlative signaling pathways of ES. The hub genes that might be therapeutic targets were also determined. In the end, we performed a CMap analysis and found several bioactive compounds that might be potential therapeutic agents for ES.

Methods

Microarray data

In this present study, the gene expression profiling datasets (GSE45544) and gene methylation profiling datasets (GSE118872) were downloaded from Gene Expression Omnibus (GEO, https://www.ncbi.nlm.nih.gov/geo/) of the National Center for Biotechnology Information (NCBI). 21 ES and 22 normal samples were included in GSE45544 (platform: GPL6244 Affymetrix Human Gene 1.0 ST Array). Twenty-one ES and 3 normal samples were included in GSE118872 (platform: GPL8490 Illumina Human Methylation 27 Bead Chip).

Data processing

GEO2R, an R-based tool provided in GEO, was used to analyze original submitted data from microarrays. DEGs and DMGs were identified with the criteria of $P < 0.05$ and $|t| > 2$. Subsequently, we obtained hypomethylated-upregulated genes by overlapping hypomethylated and upregulated genes, and by taking the intersection of hypermethylated and downregulated genes, we obtained hypermethylated-downregulated genes.

GO and KEGG enrichment analysis

Functional and pathway enrichment analysis was conducted through the Database for Annotation, Visualization, and Integrated Discovery (DAVID, https://david.ncifcrf.gov/)[10]. Gene ontology (GO) elucidates the roles of the selected genes in three aspects: molecular function, biological process, and cellular component[11]. Kyoto Encyclopedia of Genes and Genomes (KEGG) pathway enrichment analysis of selected genes was performed to identify important pathways. P-value < 0.05 was considered significant.

Protein-protein interaction (PPI) network construction and module analysis

To demonstrate the interaction between identified genes, the PPI network was built in the Search Tool for the Retrieval of Interacting Genes (STRING) database with the criteria of an interaction score ≥0.4. For further analysis, the network was visualized in Cytoscape, an open-source software platform for visualizing complex networks. Molecular Complex Detection (MCODE), an app for cluster analysis in Cytoscape, was used to find important functional modules of selected genes. Degree cut off=2, node score cut off=0.2, k-score=2, and max depth=100 were regarded as significant. CytoHubba, an app in Cytoscape, was used to identify hub genes with the Matthews Correlation Coefficient (MCC) algorithm, and node=5 were set as the criterion.

Identification of small-molecule compounds by CMap analysis

The Connectivity Map (CMap), a gene-expression based drug development database, makes it efficient for researchers to find potential agents that might reverse transcriptional profiles of relevant diseases[12]. For CMap analysis, the hub genes were converted into probes and subsequently submitted to the “query” section. P-value <0.01 and enrichment score<0 were set as screening criteria.

Results

Identification ofabnormallymethylatedanddifferentiallyexpressedgenes in ES

To find DEGs or DMGs, we used GEO2R to analyze the corresponding profiling datasets. We then identified 1876 upregulated genes and 6805 downregulated genes from the gene expression microarray (GSE45544). We also obtained 843 hypomethylated genes as well as 1503 hypermethylated genes from gene methylation profiling microarrays (GSE118872). Subsequently, by overlapping 1876 upregulated DEGs and the 843 hypomethylated DMGs, a total of 135 hypomethylated-upregulated genes were gained. Similarly, by taking the intersection of 6805 downregulated DEGs and 1503 hypermethylated DMGs, we obtained 523 hypermethylated-downregulated genes (Fig 1).

GO and KEGG enrichment analysis

To picture the attributes of the genes found above, we played GO and KEGG enrichment analysis through DAVID. For hypomethylated-upregulated genes, we found that the molecular functions (MFs) of those genes were enriched in calcium ion binding, oxidoreductase activity, and serine-type endopeptidase

inhibitor activity. As for biological processes (BPs), these genes indicated enrichment in intracellular signal transduction and positive regulation of the apoptotic process. For cell components (CCs), the analysis suggested enrichment mainly focused on extracellular regions. It indicated hypomethylated-upregulated genes might function in the tumor microenvironment of ES. Hypomethylated-upregulated genes might significantly act in some pathways, including metabolic pathways, phagosomes, and peroxisome proliferators-activated receptors (PPAR) signaling pathways (Fig 2).

For hypermethylated-downregulated genes, molecular function enrichment indicated protein binding, DNA binding, and structural constituents of the ribosome. Enriched biological processes included cell division, apoptotic process, and transcription from the RNA polymerase II promoter. Additionally, enriched cell components included the nucleus and nucleoplasm, cytosol and cytoplasm. For hypermethylated-downregulated genes, the KEGG analysis suggested enrichment of those genes in pyrimidine metabolism, cell cycle, purine metabolism, and ubiquitin-mediated proteolysis (Fig 3).

PPI network construction, module analysis and hub gene selection

To identify the relationships between hypomethylated-upregulated genes, this study conducted PPI network analysis according to the STRING database. The results were visualized in Cytoscape and are shown in Fig 4A. We then performed an MCODE analysis in Cytoscape. Three important modules were obtained and are displayed in Fig 4B-D. The top 5 hub genes were *C3*, *TF*, *PNPLA2*, *VWA1,* and *FUCA2*(Fig 6A). We analyzed hypermethylated-downregulated genes in the same way then the PPI network is displayed in Fig 5A, and three important modules are illustrated in Fig 5B-D. The top 5 hub genes were *CDC20*, *TCEB1*, *CUL2*, *ASB6,* and *KLHL13* (Fig 6B).

CMap analysis

Using the CMap database, we found a total of 6 bioactive compounds that might exert therapeutic effects on Ewing's sarcoma, including iloprost, prednisolone, diphenhydramine, butacaine, benzbromarone, fendiline, as shown in Table 1. Among them, iloprost, benzbromarone, and fendiline were reported with an obvious anti-tumor effect. The others including prednisolone and diphenhydramine were usually combined with other drugs for tumor clinical treatment.

Discussion

Despite progress in the treatment of ES, the survival rate of ES remains poor[13]. Most patients diagnosed with ES have a chromosomal translocation[14]. Some researchers have reported that chromosomal translocation can facilitate widespread epigenetic alterations[15]. Therefore, it is essential to elucidate the underlying epigenetic changes in ES.

For hypomethylated-upregulated genes, GO enrichment analysis demonstrated that the biological processes were associated with intracellular signal transduction, proteolysis, and positive regulation of apoptotic processes. This is reasonable because previous studies have demonstrated that both altered

signal transduction cascades and evasion of apoptosis are hallmarks of cancers, including ES[16, 17]. PARP proteolysis has been found in the process of apoptosis in Ewing's sarcoma[18]. KEGG pathway enrichment analysis showed several significantly enriched pathways including arginine and proline metabolism, the PPAR signaling pathway, and pertussis. The PPAR signaling pathway has been reported to be involved in a variety of cancers, but its specific function is unclear[19]. Some researchers believe that PPAR pathway activation could promote the initiation or development of tumors, while others hold the opposite opinion[20]. Arginine and proline are two important nonessential amino acids, and their synthesis could promote tumor growth[21]. Besides, pertussis toxin can influence the stimulation and inhibition of adenylate cyclase, which plays an important role in Ewing's sarcoma activities[22].

Besides, the PPI network illustrated the functional connections between gene expression and gene methylation in ES. Through Cytoscape, the top 5 hub genes were presented: *C3*, *TF*, *PNPLA2*, *VWA1*, and *FUCA2*. The *C3* gene encodes complement C3, which is a central protein associated with most complement activation pathways, and the *C3* gene is a direct target of PPAR receptor α, which could function in certain functional pathways of ES metabolism [23, 24]. The *TF* gene encodes transferrin, an iron-binding transport protein that is usually overexpressed on the surface of tumor cells, including ES cells [25, 26], some researchers found that transferrin and its receptor were also closely associated with tumor cell growth and proliferation[27]. The *PNPLA2* gene encodes a protein named adipose triglyceride lipase, which is expressed in human tumors and related to tumor aggressiveness [28]. The *VWA1* gene encodes von Willebrand factor A-domain-related protein (WARP), the function of which is still unclear[29]. However, there is translational upregulation of VWA1 in hepatocellular carcinoma (HCC), and cell proliferation can be inhibited after knockdown of VWA1[30]. The expression of the *FUCA2* can be upregulated by interferon-gamma (IFN-γ), which is closely associated with the initiation and development of tumours[31]. However, little is known about its function in Ewing sarcoma.

For hypermethylated-downregulated genes, GO enrichment analysis demonstrated that the biological processes as cell division, apoptotic process, transcription from the RNA polymerase II promoter, and DNA replication. Molecular function enrichment included protein binding, DNA binding, poly (A) RNA binding and structural constituent of ribosome. KEGG analysis showed that the enriched pathways were pyrimidine metabolism, cell cycle, purine metabolism, and ubiquitin-mediated proteolysis. These results implied the important role of DNA replication and transcription dysregulation in the development of ES, which might be regulated by DNA methylation[32].

After the construction of the PPI network, the top 5 hub genes were identified through Cytoscape: *CDC20*, *TCEB1*, *CUL2*, *ASB6*, and *KLHL13*. *CDC20* is important in the regulation of cell cycle, and its expression is upregulated in a variety of malignant tumors [33, 34]. Hypoxia-inducible factor-1α (HIF-1α) was found to directly bind to the ES-FLI-1 promoter and could be closely related to the invasiveness of Ewing sarcoma, while TCEB1 could increase HIF stabilization [35, 36]. Thus, TCEB1 targeted drug might be helpful for ES treatment. The *CUL2* gene is believed to be a candidate tumor suppressor gene, and the protein it encodes

is a member of the cullin family, which is participated in ubiquitination and degradation of certain cellular proteins [37, 38]. The *ASB6* gene encodes a kind of ankyrin repeat protein that contains a C-terminal suppressor of cytokines signaling (SOCS) box motif, and the SOCS functions in ubiquitination and proteasomal degradation of certain proteins[39]. The Kelch domain-containing protein encoded by *KLHL13* was found to be associated with cytoskeletal functions[40]. The role of ASB6 and KLHL13 in the development of ES requires further exploration.

CMap database is commonly used for drug development. In this study, based on CMap analysis, we determined 6 small-molecule compounds that might be potential treatment options for ES. Iloprost has been shown of the highest significance among our results. As a prostaglandin analog, Iloprost has antithrombotic, vasodilatation, and cytoprotection effects[41]. In some malignant tumors, increased platelets were frequently observed, and researchers speculated that those platelets played a critical role in tumor invasion and metastasis[42]. Some preclinical studies demonstrated Iloprost could reduce adhesion of tumor cells to platelets, inhibit tumor angiogenesis, and hematogenous spread[43]. Thus, iloprost might be a potential tumor inhibitor for clinical use. Benzbromarone was also reported with an anti-tumor effect. It might influence the motility of vascular endothelial cells, and subsequently inhibit tumor angiogenesis[44]. Fendiline was FDA approved. Recent studies showed fendiline could influence multiple tumor phenotypes, including proliferation, migration, invasion, and independent growth[45].

In this study, several limitations should be acknowledged. First, we only analyzed two datasets, and a larger sample size is required to verify our results. Also, cell and animal experiments are demanded to further examine the effects of the filtered hub genes and associated pathways on ES. Analysis of clinical parameters and prognosis is also lacking due to the limitations of data. Therefore, further experiments are indispensable to verify the specific function of methylation and hub genes in ES.

Conclusion

In a word, this study identified abnormally methylated-differentially expressed genes and their roles in ES using bioinformatics tools. Besides, we identified 10 hub genes, among them, C3, TF, and TCEB1 might be potential therapeutic targets for ES. The 6 identified bioactive compounds might provide some novel insights for ES treatment.

Declarations

Ethics approval and consent to participate

Not applicable

Consent for publication

Not applicable

Availability of data and materials

Not applicable

Competing interests

The authors declare that they have no competing interests.

Funding

This work was supported by a grant from the following funding: National Natural Science Foundation of China (81620108018, 81930070, 81902216), Tianjin key research and development plan, key projects for science and technology support (19YFZCSY00660).

Authors' contributions

Shijie Gao, Guowang Li and Hao Yu collected the data and performed the analysis; Shijie Gao, Guowang Li, and Hao Yu wrote the paper; Guangzhi Ning and Wendong Ruan conceived the study. All authors read and approved the final manuscript.

Acknowledgements

Thanks for technical help and writing assistance of Shiyang Yuan, Wenxiang Li, Ziqian Xiang.

References

1. Hoang NT, Acevedo LA, Mann MJ, Tolani B. A review of soft-tissue sarcomas: translation of biological advances into treatment measures. Cancer Manag Res. 2018;10:1089–114.
2. Ren C, Ren T, Yang K, Wang S, Bao X, Zhang F, et al. Inhibition of SOX2 induces cell apoptosis and G1/S arrest in Ewing's sarcoma through the PI3K/Akt pathway. J Exp Clin Cancer Res. 2016;35:44.
3. Xiao X, Garbutt CC, Hornicek F, Guo Z, Duan Z. Advances in chromosomal translocations and fusion genes in sarcomas and potential therapeutic applications. Cancer treatment reviews. 2018;63:61–70.
4. Williams RF, Fernandez-Pineda I, Gosain A. Pediatric Sarcomas. Surg Clin North Am. 2016;96(5):1107–25.
5. Li Z, Yu X, Shen J, Wu WK, Chan MT. MicroRNA expression and its clinical implications in Ewing's sarcoma. Cell Prolif. 2015;48(1):1–6.
6. Cavalli G, Heard E. Advances in epigenetics link genetics to the environment and disease. Nature. 2019;571(7766):489–99.

7. Maiuri AR, O'Hagan HM. Interplay Between Inflammation and Epigenetic Changes in Cancer. Prog Mol Biol Transl Sci. 2016;144:69–117.
8. Kim M, Costello J. DNA methylation: an epigenetic mark of cellular memory. Exp Mol Med. 2017;49(4):e322.
9. Park HR, Jung WW, Kim HS, Park YK. Microarray-based DNA methylation study of Ewing's sarcoma of the bone. Oncology letters. 2014;8(4):1613–7.
10. Dennis G, Sherman BT, Hosack DA, Yang J, Gao W, Lane HC, et al. DAVID: Database for Annotation, Visualization, and Integrated Discovery. Genome biology. 2003;4(5):P3.
11. The Gene Ontology (GO). project in 2006. Nucleic acids research. 2006;34(Database issue):D322-6.
12. <cmar-10-1089.pdf>.
13. Yu H, Ge Y, Guo L, Huang L. Potential approaches to the treatment of Ewing's sarcoma. Oncotarget. 2017;8(3):5523–39.
14. Ryan JJ, Sprunger ML, Holthaus K, Shorter J, Jackrel ME. Engineered protein disaggregases mitigate toxicity of aberrant prion-like fusion proteins underlying sarcoma. J Biol Chem. 2019;294(29):11286–96.
15. Riggi N, Cironi L, Stamenkovic I. Synovial sarcoma: when epigenetic changes dictate tumour development. Swiss Med Wkly. 2018;148:w14667.
16. Ye Q, Liu J, Xie K. Zinc finger proteins and regulation of the hallmarks of cancer. Histology histopathology. 2019;34(10):1097–109.
17. Villanova L, Careccia S, De Maria R, Fiori ME. Micro-Economics of Apoptosis in Cancer: ncRNAs Modulation of BCL-2 Family Members. International journal of molecular sciences. 2018;19(4).
18. Soldatenkov V, Notario V, Dritschilo A. Expression of the human Bcl-2 increases resistance of Ewing's sarcoma cells to apoptosis and inhibits poly(ADP-ribose) polymerase cleavage induced by radiation. Int J Oncol. 1996;9(3):547–51.
19. Peters JM, Foreman JE, Gonzalez FJ. Dissecting the role of peroxisome proliferator-activated receptor-β/δ (PPARβ/δ) in colon, breast, and lung carcinogenesis. Cancer Metastasis Rev. 2011;30(3–4):619–40.
20. Zhang X, Yao J, Shi H, Gao B, Zhang L. LncRNA TINCR/microRNA-107/CD36 regulates cell proliferation and apoptosis in colorectal cancer via PPAR signaling pathway based on bioinformatics analysis. Biological chemistry. 2019;400(5):663–75.
21. Geck RC, Toker A. Nonessential amino acid metabolism in breast cancer. Advances in biological regulation. 2016;62:11–7.
22. van Valen F, Keck E, Jürgens H. Neuropeptide Y inhibits vasoactive intestinal peptide- and dopamine-induced cyclic AMP formation in human Ewing's sarcoma WE-68 cells. FEBS Lett. 1989;249(2):271–4.
23. Walport MJ. Complement. First of two parts. N Engl J Med. 2001;344(14):1058–66.

24. Mogilenko DA, Kudriavtsev IV, Shavva VS, Dizhe EB, Vilenskaya EG, Efremov AM, et al. Peroxisome proliferator-activated receptor α positively regulates complement C3 expression but inhibits tumor necrosis factor α-mediated activation of C3 gene in mammalian hepatic-derived cells. J Biol Chem. 2013;288(3):1726–38.
25. Gatter KC, Brown G, Trowbridge IS, Woolston RE, Mason DY. Transferrin receptors in human tissues: their distribution and possible clinical relevance. J Clin Pathol. 1983;36(5):539–45.
26. Hu-Lieskovan S, Heidel JD, Bartlett DW, Davis ME, Triche TJ. Sequence-specific knockdown of EWS-FLI1 by targeted, nonviral delivery of small interfering RNA inhibits tumor growth in a murine model of metastatic Ewing's sarcoma. Cancer research. 2005;65(19):8984–92.
27. Shen Y, Li X, Dong D, Zhang B, Xue Y, Shang P. Transferrin receptor 1 in cancer: a new sight for cancer therapy. American journal of cancer research. 2018;8(6):916–31.
28. Wang YY, Attané C, Milhas D, Dirat B, Dauvillier S, Guerard A, et al. Mammary adipocytes stimulate breast cancer invasion through metabolic remodeling of tumor cells. JCI insight. 2017;2(4):e87489.
29. Fitzgerald JWARP: A Unique Extracellular Matrix Component of Cartilage, Muscle, and Endothelial Cell Basement Membranes. Anatomical record (Hoboken, NJ: 2007). 2019.
30. Zou Q, Xiao Z, Huang R, Wang X, Wang X, Zhao H, et al. Survey of the translation shifts in hepatocellular carcinoma with ribosome profiling. Theranostics. 2019;9(14):4141–55.
31. Sobkowicz AD, Gallagher ME, Reid CJ, Crean D, Carrington SD, Irwin JA. Modulation of expression in BEAS-2B airway epithelial cells of α-L-fucosidase A1 and A2 by Th1 and Th2 cytokines, and overexpression of α-L-fucosidase 2. Molecular cellular biochemistry. 2014;390(1–2):101–13.
32. Goss KL, Gordon DJ. Gene expression signature based screening identifies ribonucleotide reductase as a candidate therapeutic target in Ewing sarcoma. Oncotarget. 2016;7(39):63003–19.
33. Yang WL, Li J, An P, Lei AM. CDC20 downregulation impairs spindle morphology and causes reduced first polar body emission during bovine oocyte maturation. Theriogenology. 2014;81(4):535–44.
34. Gayyed MF, El-Maqsoud NMRA, Tawfiek ER, El Gelany SAA, Rahman MFA. A comprehensive analysis of CDC20 overexpression in common malignant tumors from multiple organs: its correlation with tumor grade and stage. Tumour Biol. 2016;37(1):749–62.
35. Hameiri-Grossman M, Porat-Klein A, Yaniv I, Ash S, Cohen IJ, Kodman Y, et al. The association between let-7, RAS and HIF-1α in Ewing Sarcoma tumor growth. Oncotarget. 2015;6(32):33834–48.
36. Batavia AA, Schraml P, Moch H. Clear cell renal cell carcinoma with wild-type von Hippel-Lindau gene: a non-existent or new tumour entity? Histopathology. 2019;74(1):60–7.
37. Clifford SC, Walsh S, Hewson K, Green EK, Brinke A, Green PM, et al. Genomic organization and chromosomal localization of the human CUL2 gene and the role of von Hippel-Lindau tumor suppressor-binding protein (CUL2 and VBP1) mutation and loss in renal-cell carcinoma development. Genes Chromosomes Cancer. 1999;26(1):20–8.
38. Kipreos ET, Lander LE, Wing JP, He WW, Hedgecock EM. cul-1 is required for cell cycle exit in C. elegans and identifies a novel gene family. Cell. 1996;85(6):829–39.

39. Linossi EM, Nicholson SE. The SOCS box-adapting proteins for ubiquitination and proteasomal degradation. IUBMB Life. 2012;64(4):316–23.
40. Sumara I, Quadroni M, Frei C, Olma MH, Sumara G, Ricci R, et al. A Cul3-based E3 ligase removes Aurora B from mitotic chromosomes, regulating mitotic progression and completion of cytokinesis in human cells. Dev Cell. 2007;12(6):887–900.
41. Pountos I, Giannoudis PV. The role of Iloprost on bone edema and osteonecrosis: Safety and clinical results. Expert Opin Drug Saf. 2018;17(3):225–33.
42. Kanikarla-Marie P, Lam M, Menter DG, Kopetz S. Platelets, circulating tumor cells, and the circulome. Cancer Metastasis Rev. 2017;36(2):235–48.
43. Schneider MR, Schillinger E, Schirner M, Skuballa W, Stürzebecher S, Witt W. Effects of prostacyclin analogues in in vivo tumor models. Adv Prostaglandin Thromboxane Leukot Res. 1991;21B:901–8.
44. Tadjuidje E, Wang TS, Pandey RN, Sumanas S, Lang RA, Hegde RS. The EYA tyrosine phosphatase activity is pro-angiogenic and is inhibited by benzbromarone. PLoS ONE. 2012;7(4):e34806.
45. Woods N, Trevino J, Coppola D, Chellappan S, Yang S, Padmanabhan J. Fendiline inhibits proliferation and invasion of pancreatic cancer cells by interfering with ADAM10 activation and β-catenin signaling. Oncotarget. 2015;6(34):35931–48.

Tables

Table 1: Results of CMap analysis

Rank	CMap name	Mean	N	Enrichment	P-value
1	iloprost	-0.823	3	-0.964	0.00012
2	prednisolone	-0.371	5	-0.773	0.00106
3	diphenhydramine	-0.444	5	-0.747	0.00192
4	butacaine	-0.35	4	-0.776	0.00515
5	benzbromarone	-0.642	3	-0.834	0.00899
6	fendiline	-0.605	3	-0.831	0.00973

Figures

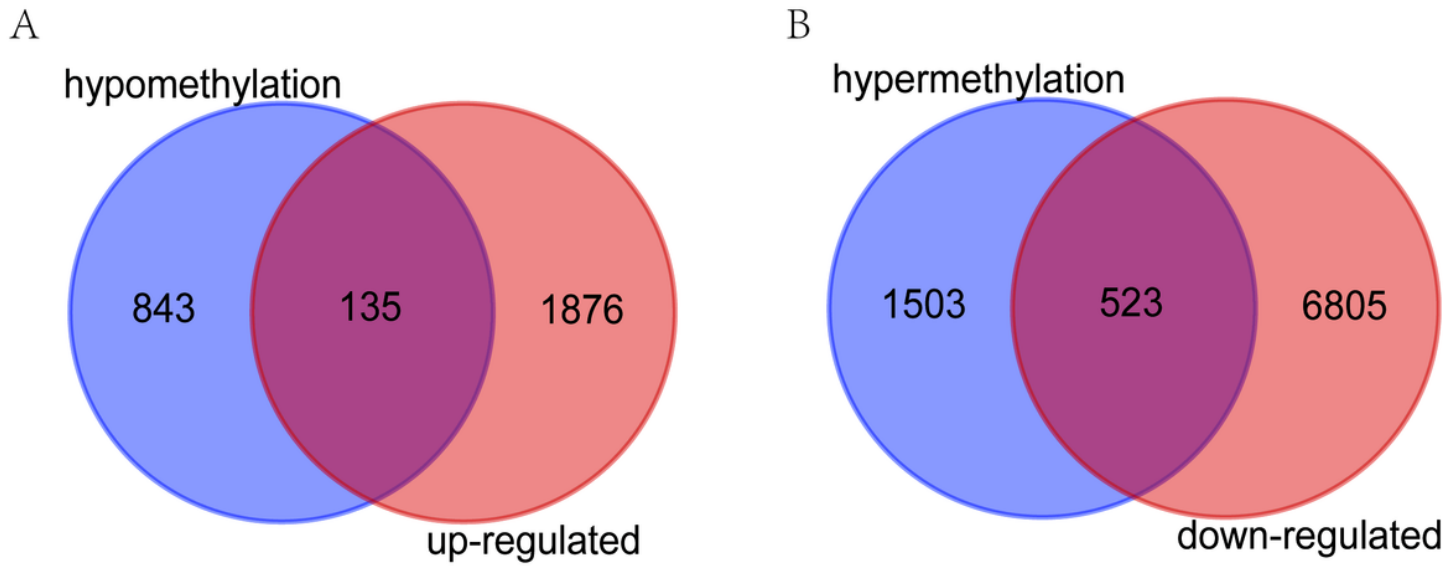

Figure 1

Venn diagrams showing the aberrantly methylated-differently expressed genes from gene expression microarrays (GSE45544) and gene methylation microarrays (GSE118872) Fig 1A: Hypomethylated and upregulated genes. Fig 1B: Hypermethylated and downregulated genes.

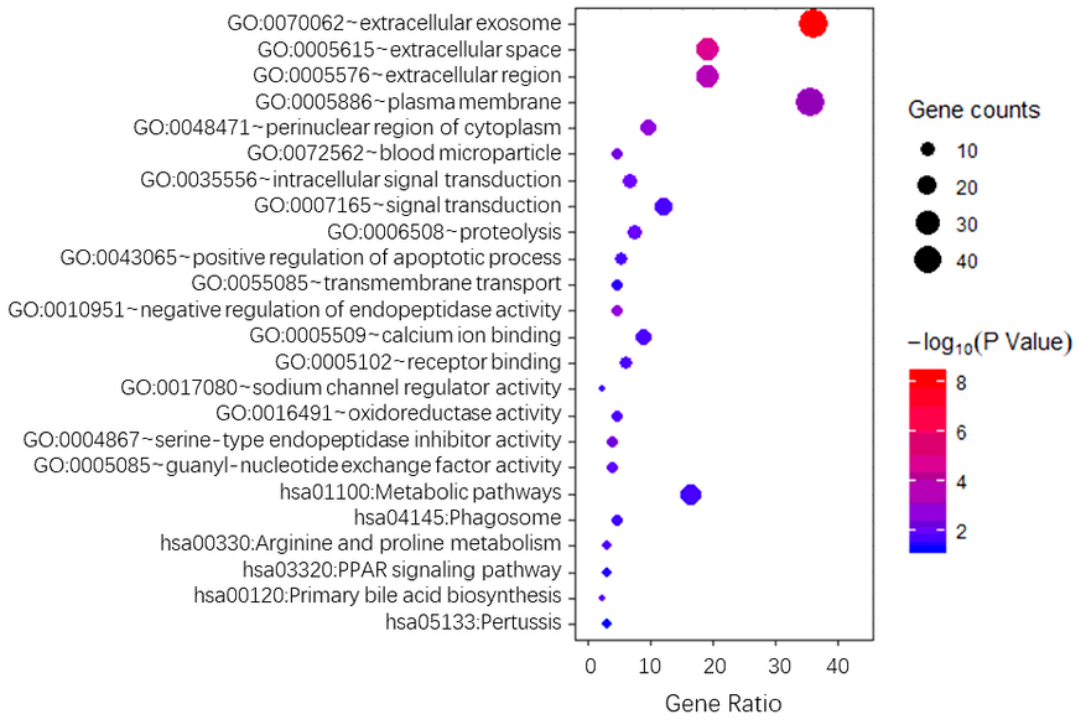

Figure 2

GO and KEGG enrichment analysis of hypomethylated and upregulated genes in ES.

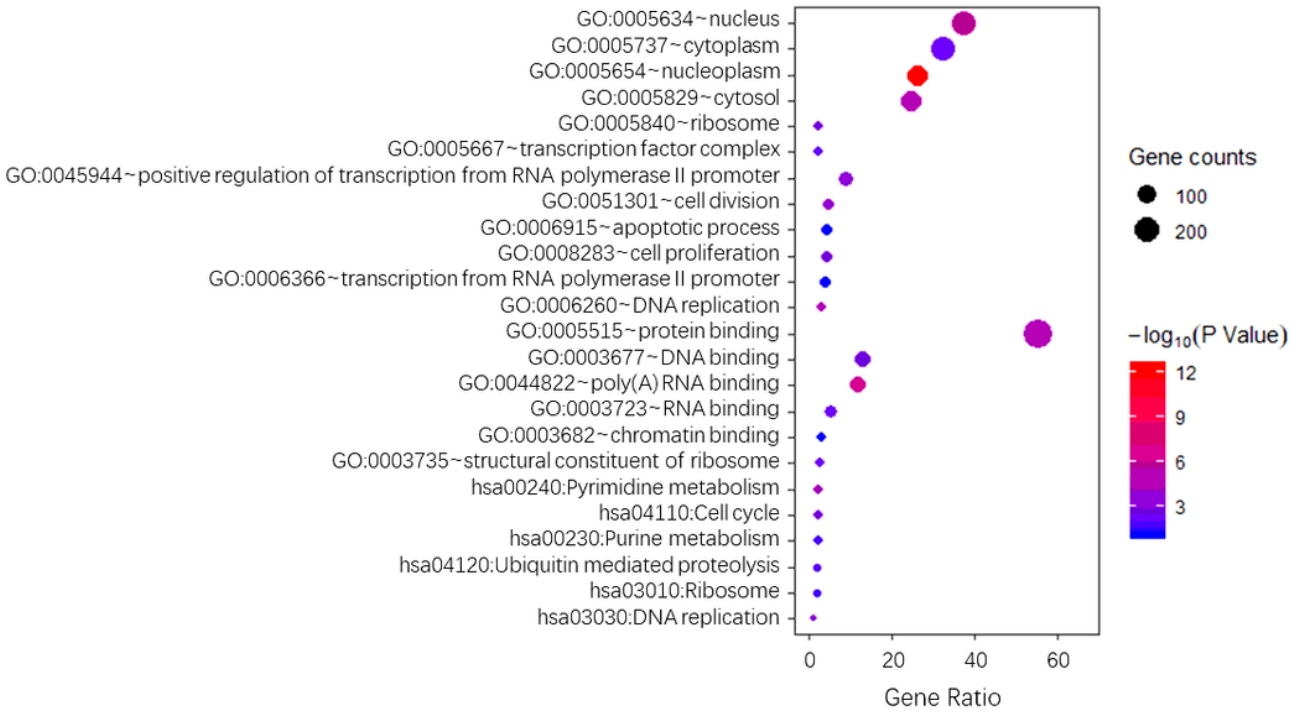

Figure 3

GO and KEGG enrichment analysis of hypermethylated and downregulated genes in ES.

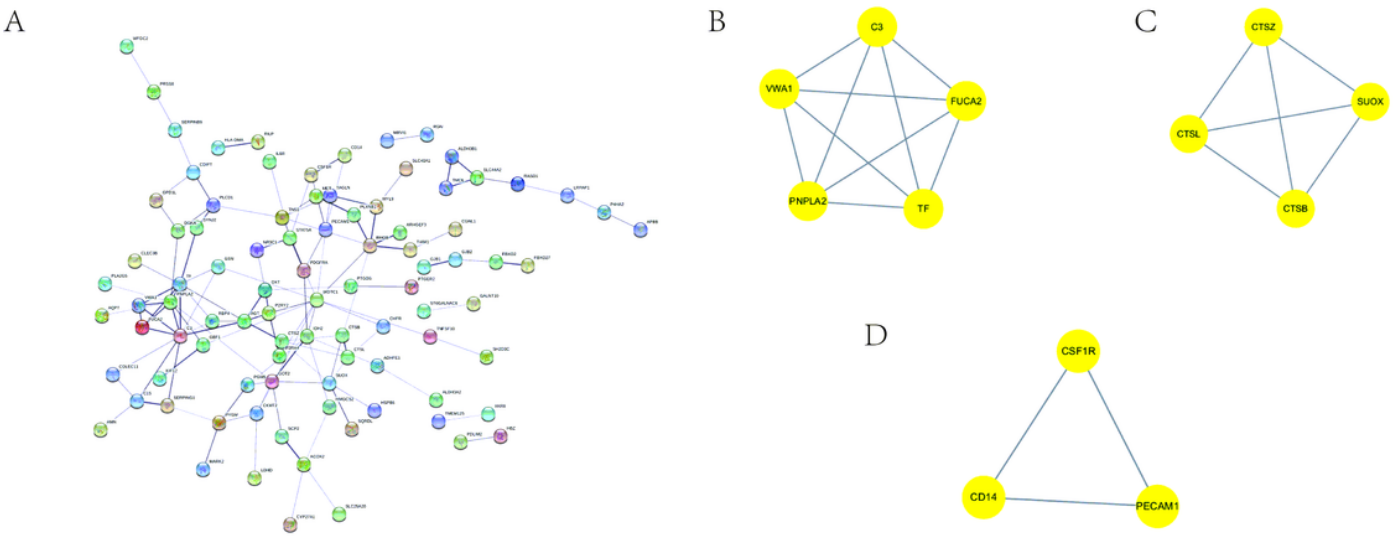

Figure 4

PPI network of hypomethylated-upregulated genes and three modules. Fig 4A: PPI network. Fig 4B: Top 1 module. Fig 4C: Top 2 module. Fig 4D: Top 3 module.

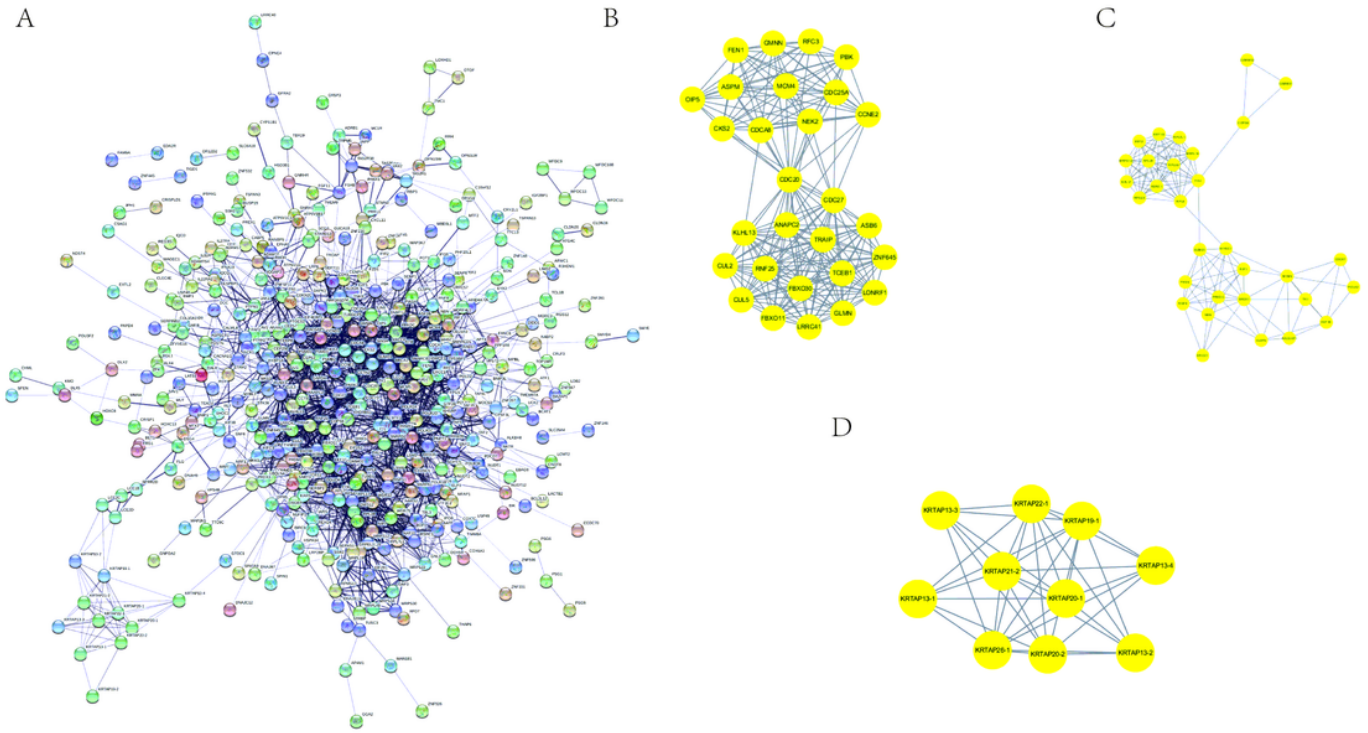

Figure 5

PPI network of hypermethylated-downregulated genes and three modules. Fig 5A: PPI network. Fig 5B: Top 1 module. Fig 5C: Top 2 module. Fig 5D: Top 3 module.

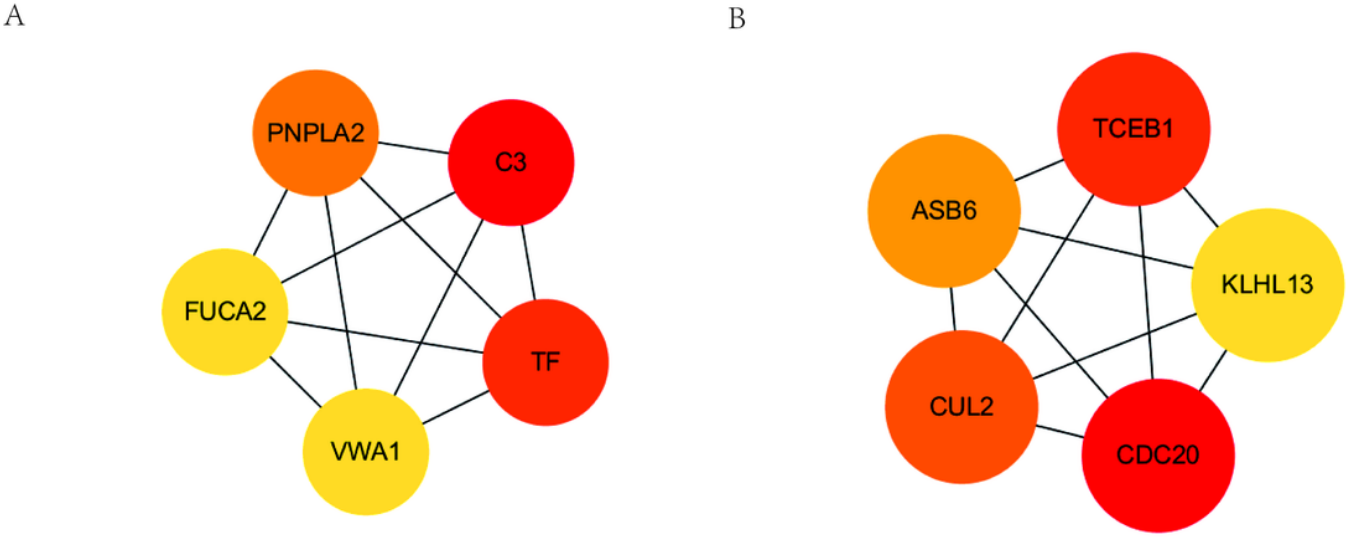

Figure 6

Hub genes of aberrantly methylated-differently expressed genes in ES. Fig 6A: 5 hub genes of hypomethylated-upregulated genes. Fig 6B: 5 hub genes of hypermethylated-downregulated genes.